압전센서를 이용하는 철로에서의 손상 검색 기술

Damage Detection of Railroad Tracks Using Piezoelectric Sensors

윤 정 방* · 박 승 희** · 다니엘 인만***

Yun, Chung-Bang · Park, Seunghee · Inman, Daniel J.

ABSTRACT

Piezoelectric sensor-based health monitoring technique using a two-step support vector machine (SVM) classifier is discussed for damage identification of a railroad track. An active sensing system composed of two PZT patches was investigated in conjunction with both impedance and guided wave propagation methods to detect two kinds of damage of the railroad track (one is a hole damage of 0.5cm in diameter at web section and the other is a transverse cut damage of 7.5cm in length and 0.5cm in depth at head section). Two damage-sensitive features were extracted one by one from each method; a) feature I: root mean square deviations (RMSD) of impedance signatures and b) feature II: wavelet coefficients for A_0 mode of guided waves. By defining damage indices from those damage-sensitive features, a two-dimensional damage feature (2-D DF) space was made. In order to minimize a false-positive indication of the current active sensing system, a two-step SVM classifier was applied to the 2-D DF space. As a result, optimal separable hyper-planes were successfully established by the two-step SVM classifier: Damage detection was accomplished by the first step-SVM, and damage classification was also carried out by the second step-SVM. Finally, the applicability of the proposed two-step SVM classifier has been verified by thirty test patterns.

Keywords: *Piezoelectric Sensors (PZT), Structural Health Monitoring, Impedance, Guided Waves, RMSD, Wavelet Analysis, Support Vector Machines, Railroad Tracks.*

1. Introduction

It has been reported that train accidents caused by railroad track failures resulted in 2700 derailments and $302million in direct costs during the decade 1992-2002 ($48million in the year 2001 alone) (US federal railroad administration 2002). The main causes of these accidents have proved to be deteriorating condition of aging rail tracks. A recent example is the derailment accident on Chicago's south side in September 17, 2005, shown in Figure 1. In order to prevent similar accidents, a smart monitoring system including low-cost but high-effect smart sensors such as piezoelectric sensors, optical fiber sensors, and micro-electromechanical system (MEMS) sensors and wireless risk alarming systems is being investigated. Conventionally, magnetic or ultrasonic transducer-based techniques have been used for railroad track inspection (Clark *et al.* 2004, Grewal *et al.* 1996, and Cawley *et al.* 2003). However, those techniques usually require a direct access to the structure and involve bulky equipment. Moreover, those techniques require disruptions of the operation of the structure/equipment, which is not attractive for real world-application. Therefore, this study introduces an active sensing system composed of two PZT patches in conjunction with both impedance and guided wave propagation methods for damage detection of the railroad track. Two damage-sensitive features were extracted one by one from each method. By defining damage indices from those two damage-sensitive features, a two-dimensional damage feature (2-D DF) space has been made. Furthermore, a two-step SVM classifier was newly applied to the 2-D DF space. Finally, the applicability of the proposed two-step SVM classifier has been verified.

2. Piezoelectric Sensor-based SHM Techniques

Piezoelectric sensors, which are shown in Figure 2, can be used as both actuators and sensors at the same time. When an electric field is applied to the piezoelectric material, the material produces mechanical strains proportional to the electrical field (actuators). Conversely, when mechanical pressure is applied, the material obtains voltage proportional to the pressure (sensors). The following constitutive equations describe the effects of the piezoelectric materials:

* 정회원 · 한국과학기술원 건설 및 환경공학과 교수 E-mail: ycb@kaist.ac.kr

** 한국과학기술원 건설 및 환경공학과 박사과정 E-mail: shparkpc@kaist.ac.kr

*** Professor, Dept. of Mechanical Engineering, Virginia Tech, E-mail: dinman@vt.edu

$$S_{ij} = s^E_{ijkl} T_{kl} + d_{kij} E_k \quad (1)$$

$$D_i = d_{ikl} T_{kl} + \varepsilon^T_{ik} E_k \quad (2)$$

where S_{ij} is a mechanical strain, T_{kl} is a mechanical stress, E_k is an applied electric field, D_i is a dielectric displacement, s^E_{ijkl} is a mechanical compliance (at constant electric field), ε^T_{ik} is a dielectric permittivity (at constant mechanical stress), and d_{kij} is a piezoelectric constant. Based on this functionality, piezoelectric ceramic lead-zirconate-titanate (PZT) patches have been the most widely used in SHM fields (Giurgiutiu and Rogers 1997, Park *et al.* 2000, Park *et al.* 2005, Giurgiutiu *et al.* 2003, and Raghavan *et al.* 2004). There are two kinds of significant PZT-based SHM methods: (a) impedance-based damage detection method, and (b) guided wave propagation-based damage detection method.

2.1. Impedance-based Damage Detection Techniques

The coupling effect of the electro-mechanical impedance of a system with PZT and a host structure can be conceptually investigated as shown in Figure 3 (Giurgiutiu and Rogers 1997). The integrated electro-mechanical system may be electrically represented by the electrical impedance which is affected by the dynamics of the PZT and the host structure given by (Giurgiutiu and Rogers 1997)

$$Z_{total}(\omega) = [i\omega C(1 - \kappa^2_{31} \frac{Z_s(\omega)}{Z_A(\omega) + Z_s(\omega)})]^{-1} \quad (3)$$

where C is the zero-load capacitance of the PZT and κ_{31} is the electromechanical coupling coefficient of the PZT. The electro-mechanical impedance technique permits damage detection, health monitoring, and *built-in* NDE because it can measure directly the high frequency local impedance which is very sensitive to local damage. In other words, changes of the mechanical properties of the host structure may be detected by monitoring the variations of the electro-mechanical impedance functions shown in Equation (3). Experimental setup for the impedance-based damage detection techniques consists of an impedance analyzer (HP4194A), a personal computer which can control Matlab programs for data acquisition, signal processing and damage diagnosis, and a *built-in* PZT patch structural system, as illustrated in Figure 4. For damage quantifications of the impedance-based damage detection technique, root mean square deviations (RMSD) of the impedance signatures would be considered as a damage indicator, which is given by

$$RMSD(\%) = \sqrt{\frac{\sum_{i=1}^{i=N} (\mathrm{Re}(Z(\omega_i)) - \mathrm{Re}(Z_0(\omega_i)))^2}{\sum_{i=1}^{i=N} (\mathrm{Re}(Z_0(\omega_i)))^2}} \times 100 \quad (4)$$

where $Z(\omega_i)$ is the post-damage impedance signature at the i-th measurement point and $Z_0(\omega_i)$ is the corresponding pre-damage value. Recently, an outlier analysis (novelty detection)-based damage detection method was successfully applied to the impedance methods by Park et al. 2005. An optimal threshold value for damage detection should be determined through the outlier analysis.

2.2. Guided Wave Propagation-based Damage Detection Techniques

Lamb waves refer to elastic perturbations propagating in a solid plate with doubly free boundaries, for which displacements occur both in parallel and perpendicular to the direction of wave propagation (Viktorov *et al.*1967). There are two groups of waves, symmetric and anti-symmetric, which propagate independently of each other. A graphical representation of those two groups of waves can be seen in Figure 5. If a set of transmitting and receiving PZT patches are placed on a structure, the received signal contains information about the integrity along the wave path between two PZT patches. Therefore, the present method may be used to monitor a path rather than a point, and considerable savings in testing time may be obtained. Unfortunately, however, Lamb wave testing gets complicated by the dispersive nature of Lamb waves. Figure 5 presenting dispersion curves of Lamb waves for a steel plate shows that many wave components with different group velocities exist at the high frequency range. So, attempts have been made to limit the bandwidth of the excitation to a low frequency range over which there exist only two fundamental modes (A_0 or S_0). An investigation on the dominance of the fundamental Lamb modes over the proper frequency range for the steel members has been reported (Giurgiutiu *et al.* 2003 and Raghavan *et al.* 2004). Accordingly, the only A_0 mode is intentionally selected and investigated for the present study. Experimental setup for the guided wave propagation-based damage detection techniques consists of a function generator with an amplifier, a digital oscilloscope, a personal computer which can control Matlab programs for data acquisition, signal processing and damage diagnosis, and PZT patch *built-in* structural system, as shown in Figure 6. Wavelet analysis

would be implemented for a joint time-frequency analysis of the guided waves (Jeong *et al.* 2000). A general overview of wavelet analysis may be found in Chui *et al.* 1992. Using a selected mother wavelet function, $\psi(t)$, the continuous wavelet transform (CWT) of a signal $x(t)$ is defined as

$$(Wf)(b,a) = \int_{-\infty}^{+\infty} x(t)\frac{1}{\sqrt{a}}\psi^*(\frac{t-b}{a})dt \tag{5}$$

where continuous variables a and b are the scale and translation parameters, respectively. In the present study, a "Morlet wavelet" is employed as a mother wavelet function. Recently, wavelet-based approaches for damage detection have been reported by Staszewski *et al.* 1997 and Hou *et al.* 2000.

3. Damage Index Approach

In this study, two kinds of damage-sensitive features are utilized: a) feature I: root mean square deviations (RMSD) of impedance signatures, and b) feature II: wavelet coefficients for A_0 mode of the guided waves. From those features, appropriate damage indices would be proposed as follows:

$$\mathrm{DF}_X = \frac{\left|R^d - R^0\right|}{R^0} \tag{6}$$

$$\mathrm{DF}_Y = \frac{\left|\sum_{i=1}^{l}(C_i^d)^2 - \sum_{i=1}^{l}(C_i^0)^2\right|}{\sum_{i=1}^{l}(C_i^0)^2}, \quad l\text{: Number of data points} \tag{7}$$

where R means RMSD, C_i means wavelet coefficients of the corresponding wave mode, superscripts d and 0 mean 'after a corresponding damage step' and 'before a corresponding damage step', respectively. These damage indices will compose a two-dimensional damage feature (2-D DF) space (DF_X for x-axis and DF_Y for y-axis).

4. Damage Identification Using Two-Step Support Vector Machine Classifier

In order to minimize a false-positive indication in the 2-D DF space of the current active sensing system, the establishment of an optimal decision boundary is strongly required. For this kind of decision making problem, support vector machine (SVM) algorithm has emerged as a powerful tool (Vapnik *et al.*1995). The SVM is an automated learning system that uses a hypothesis space of linear functions in a high dimensional feature space. The simplest model is called linear SVM, and it works for data that are linearly separable in the original feature space only. In the early 1990s, nonlinear classification in the same procedure as linear SVM became possible by introducing nonlinear functions called kernel functions without being conscious of actual mapping space. This extended technique of nonlinear feature spaces is called nonlinear SVM shown in Figure 7. Assume the training sample S consisting of vectors $\mathbf{x}_i \in R^n$ with $i = 1,\ldots,N$, and each vector x_i belongs to either of two classes thus is given a label $y_i \in \{-1,1\}$. The pair of $(\mathbf{w}, b)$ defines a separating hyper-plane of equation as follows:

$$S = ((\mathbf{x}_1, y_1),\ldots,(\mathbf{x}_N, y_N)) \tag{8}$$

$$(\mathbf{w}\cdot\mathbf{x}) + b = 0 \tag{9}$$

where $\mathbf{w}$ and b are arbitrary constants.

However, Equation (9) can possibly separate any part of the feature space, therefore one needs to establish an optimal separating hyper-plane (OSH) that divides S leaving all the points of the same class on the same side, while maximizing the margin which is the distance of the closest point of S. The closest vector $\mathbf{x}_i$ is called support vector and the OSH $(\mathbf{w}', b')$ can be determined by solving an optimization problem. The resulting SVM is called maximal margin SVM. In order to relax the situation, maximal margin SVM is generalized by introducing non-negative slack variables $\xi = (\xi_1, \xi_2, \ldots, \xi_N)$ as follows:

$$\begin{aligned} &\text{Minimize} \quad d(\mathbf{w}') = \frac{1}{2}(\mathbf{w}'\cdot\mathbf{w}') + C\sum\xi_i, \\ &\text{Subject to} \quad y_i\left((\mathbf{w}'\cdot\mathbf{x}_i) + b'\right) \geq 1 - \xi_i, \quad i = 1,2,\ldots,N, \quad \xi \geq 0. \end{aligned} \tag{10}$$

The purpose of the extra term $C\sum\xi_i$, where $i = 1,\ldots,N$ is to keep under control the number of misclassified vectors.

The parameter C can be regarded as a regularization parameter. The OSH tends to maximize the minimum distance of $1/\mathbf{w}$ with small C, and minimize the number of misclassified vectors with large C. To solve the case of nonlinear decision surfaces, the OSH is carried out by nonlinearly transforming a set of original feature vectors $\mathbf{x}_i$ into a high-dimensional feature space by mapping $\Phi : \mathbf{x}_i \mapsto \mathbf{z}_i$ and then performing the linear separation. However, it requires an enormous computation of inner products $(\Phi(\mathbf{x}) \cdot \Phi(\mathbf{x}_i))$ in the high-dimensional feature space. A kernel function that satisfies the Mercer's theorem given in Equation (11) significantly reduces this process. In this study, a polynomial function machine with convolution function given in Equation (12) would be used as the kernel function.

$$(\Phi(\mathbf{x}) \cdot \Phi(\mathbf{x}_i)) = K(\mathbf{x}, \mathbf{x}_i) \tag{11}$$

$$K(\mathbf{x}_i, \mathbf{x}_j) = (\mathbf{x}_i \cdot \mathbf{x}_j + 1)^d \tag{12}$$

Some attempts to implement the SVM algorithm for structural health monitoring and damage detection have been made by Mita *et al.* 2004 and Park *et al.* 2005. They have shown the successful capabilities of the SVM algorithm for loosening bolts inspection on jointed structures. In the present study, a two-step SVM classifier is newly introduced. The first step-SVM is for discrimination of damage states from an intact state. The second step-SVM is for classification of damage types according to the location and degree of the damage.

5. Validation of the Proposed Approach through Experimental Study

An experimental study was carried out to validate the applicability of the proposed approach for health monitoring of a railroad track. A lab-size railroad track with a length of 140 cm was used as a test specimen, as shown in Figure 8. Two PZT patches of 2 cm x 2 cm were surface mounted on the sidewall of the web of the specimen. For damage scenario, two kinds of damage (one is a hole damage of 0.5cm in diameter at web section and the other is a transverse cut damage of 7.5cm in length and 0.5cm in depth at head section) were artificially inflicted in a sequence. First, the baseline signals were recorded 30 times and averaged from both impedance and guided wave methods. Impedance measurement was carried out over the frequency range of 140 kHz to 150 kHz at PZT #1. (Figure 9(a)) Concurrently, a single pair of pitch-catch guided wave propagation data with an input of 3-cycle sine waves in the magnitude of 10V at PZT #1 was recorded at PZT #2, and A_0 mode only was selected from the wavelet response signal. (Figure 9(b)) The same procedures were repeated for all damage cases. The measurement under a different sensor configuration, switched each other between PZT #1 and PZT #2 (PZT #1 ↔ PZT #2), was also performed ten times for each case. They are used as test patterns to verify the effectiveness of the proposed SVM classifier. Then, the damage-sensitive features were extracted as described in Table 1. As shown in Figure 9(a), an optimal threshold value of RMSD for damage detection was decided as 0.32 by an outlier analysis, and it is noted that feature I could not detect a hole damage. In addition, Figure 9(b) shows that feature II did not give any visible changes due to damage. In order to overcome these limitations, the proposed two-step SVM classifier was applied, as shown in Figure 10. A two-dimensional damage feature (2-D DF) space was obtained by calculating the damage indices defined in Equations (6) and (7), and optimal separable hyper-planes (OSH) for minimization of a false-positive indication were successfully established by using the two-step SVM classifier: Damage detection was performed by the first step-SVM and damage classification was also carried out by the second step-SVM. Finally, thirty test patterns prepared beforehand were investigated to verify the effectiveness of the proposed SVM classifiers. As a result, it can be observed that the SVM classifier has an excellent performance for damage identification. As illustrated in Figure 11, every output except only one test pattern yielded the same values with its own original target values (damage estimation rate of 96.67 %).

6. Conclusions

Piezoelectric sensor-based health monitoring technique using a two-step support vector machine (SVM) classifier was discussed for damage identification of a railroad track. An active sensing system composed of two PZT patches was investigated in conjunction with both impedance and guided wave-based damage detection methods to detect two kinds of damage of the railroad track (one is a hole damage of 0.5cm in diameter at web section and the other is a transverse cut damage of 7.5cm in length and 0.5cm in depth at head section). A two-dimensional damage feature (2-D DF) space was made by introducing appropriate damage-sensitive features. In order to minimize a false-positive indication of the current active sensing system, a two-step SVM classifier was newly applied to the 2-D DF space. As a result, optimal separable hyper-planes were successfully established by using the two-step SVM classifier: Damage detection was performed by the first step-SVM, and damage classification was also carried out by the second step-SVM. Finally, the applicability of the proposed SVM classifier has been verified by showing an excellent damage estimation rate of 96.67%. The present approaches provide an improved methodology for on-line health monitoring of real-world railroad structures.

Acknowledgments

The work was jointly supported by the Korea Research Foundation Grant funded by the Korean Government (MOEHRD) (KRF- 2005-213-D00092), Korea, and the Association of American Railroads (AAR), United States. This financial support was greatly appreciated.

References

Cawley, P. Lowe, M. J. S., Alleyne, D., Pavlakovic, B., and Wilcox, P. (2003) 'Practical Long Range Guided Wave Testing: Applications to Pipes and Rail', *Materials Evaluation*, **61**, 66-74.

Chui, C. K. (1992) 'Introduction to wavelets', *Academic*, San Diego.

Clark, R. (2004) 'Rail Flaw Detection: Overview and Needs for Future Development', *NDT&E International*, **37**, 111-118.

Federal Railroad Administration (2002) 'Safety Statistics Data: 1992-2002', *U.S. Department of Transportation.*

Giurgiutiu, V., and Rogers, C. A. (1997) 'Electro-mechanical (E/M) impedance method for structural health monitoring and nondestructive evaluation', *International Workshop on SHM*, 433-444, Stanford University, September 18-20, CA.

Giurgiutiu, V. (2003) 'Lamb wave generation with piezoelectric wafer active sensors for structural health monitoring', *Proceedings of the SPIE Conference on Smart Structures and Materials*, San Diego, CA, **5056**, 111-122.

Grewal, D.S. (1996) 'Improved Ultrasonic Testing of Railroad Rail for Transverse Discontinuous in the Rail Head Using Higher Order Rayleigh (M_{21}) Waves', *Materials Evaluation*, **54** (9), 983-986.

Hou, Z., Noori, M., and Amand, R. St. (2000) 'Wavelet-based approach for structural damage detection', *Journal of Engineering Mechanics*, **126** (7), 677-683.

Jeong, H., and Jang, Y. (2000) 'Wavelet analysis of plate wave propagation in composite laminates', Composite Structures, **49**, 443-450.

Mita, A., Taniguchi, R. (2004) 'Active Damage Detection Method Using Support Vector Machine and Amplitude Modulation', *Proceedings of 11th International SPIE Symposium on Smart Str. and Mat.*, San Diego, CA, **5391**, 21-29.

Park, G., Cudney, H., and Inman, D. J. (2000) 'Impedance-based health monitoring of civil structural components', *ASCE journal of Infrastructure Systems*, **6** (4), 153-160.

Park, S., Yun, C.-B., Roh, Y., and Lee, J.-J. (2005) 'Health monitoring of steel structures using impedance of thickness modes at PZT patches', *Smart Structures and Systems*, **1**(4), 339-353.

Park, S., Yun, C.-B., and Roh, Y. (2005) 'PZT-induced Lamb waves and pattern recognitions for on-line health monitoring of jointed steel plates', *Proceedings of SPIE Conference on Smart Str. and Mat.*, San Diego, CA, **5765**, 364-375.

Park, S., Inman, D. J., and Yun, C.-B. (2005) 'Defect Detection of Railroad Tracks Using Outlier Analysis of MFC-based Impedance Sensing Data', *Submitted to Engineering Structures.*

Raghavan, A. and Cesnik, C. E. S. (2004) 'Modeling of piezoelectric-based Lamb wave generation and sensing for structural health monitoring', *Proc. of the SPIE Conference on Smart Str. and Mat.*, San Diego, CA, **5391**, 419-430.

Staszewski, W. J. and Tomlinson, G. R. (1997) 'Application of the wavelet transform to fault detection in spur gear', *Mechanical Systems and Signal Processing*, **8** (3), 289–307.

Vapnik, V. N. (1995) '*The Nature of Statistical Learning Theory', Springer.*

Viktorov, I. A. (1996) 'Rayleigh and Lamb Waves-Physical Theory and Applications'.

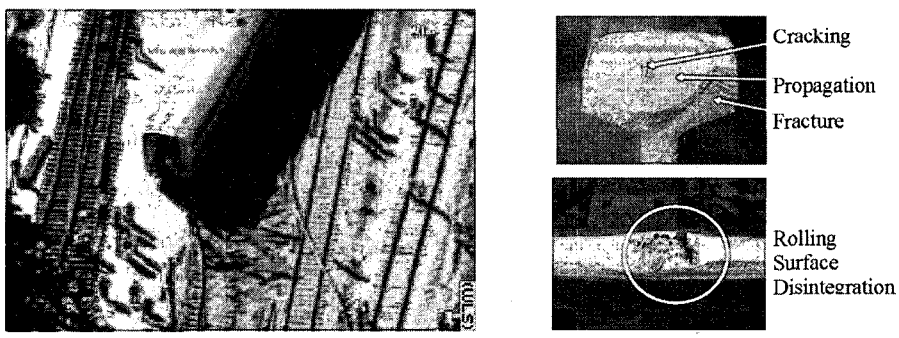

Figure 1. Derailment Accident on Chicago's South Side (Sep.17.2005,www.cnn.com) and Examples of Deterioration of Aging Rails

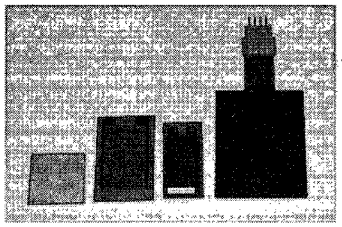

Figure 2. Piezoelectric Sensors

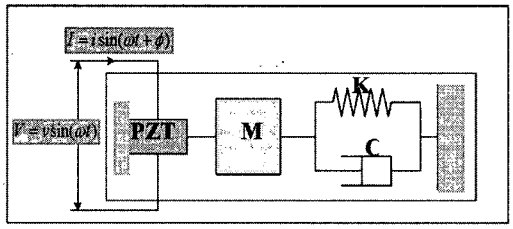

Figure 3. Electro-mechanical System between PZT and Host Structure

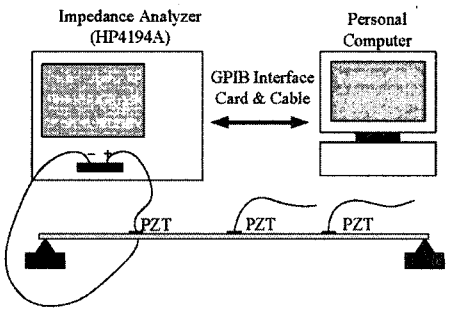

Figure 4. Experimental Setup for Impedance-based Damage Detection Techniques

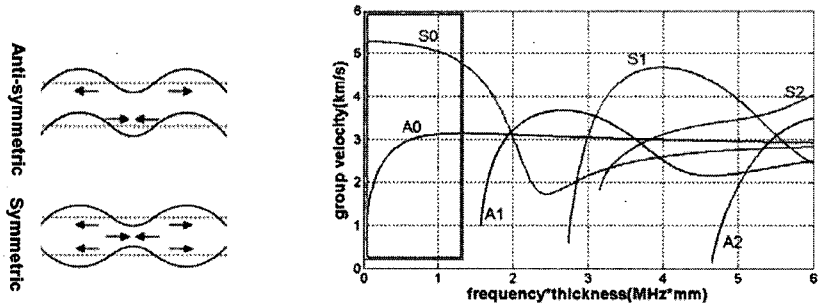

Figure 5. Dispersion Curves with Anti-symmetric and Symmetric Modes)

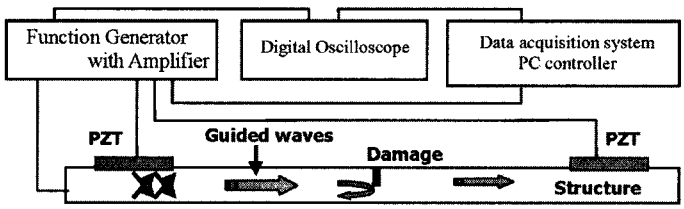

Figure 6. Experimental Setup for Guided Wave Propagation-based Damage Detection Techniques

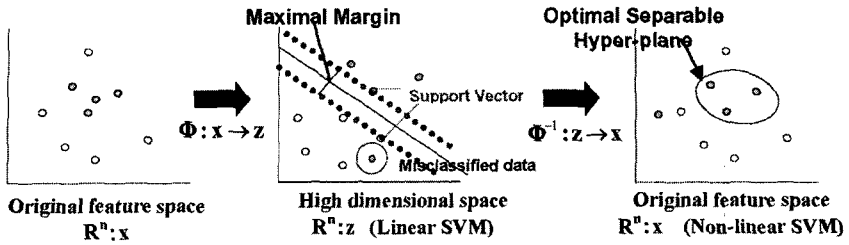

Figure 7. Non-linear Support Vector Machine (SVM)

Figure 8. Test Specimen and Damage Descriptions

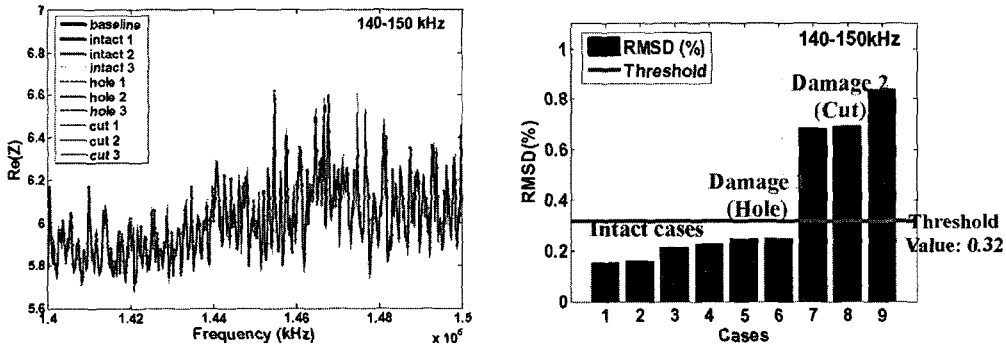

(a) Impedance Signatures and feature I: RMSD

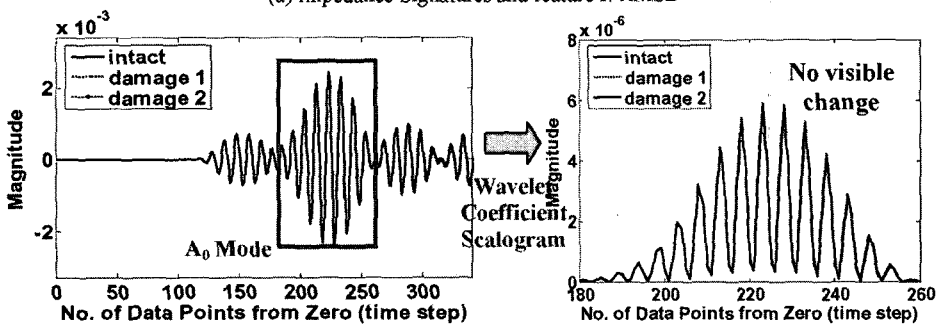

(b) Guided Waves and feature II: Wavelet Coefficients for A_0 Mode

Figure 9. Experimental Results for Impedance and Guided Wave Methods

Table 1. Damage-Sensitive Features for Intact and Damage States
(feature I: RMSD of Impedance Data and feature II: Sum of Square of Wavelet Coefficients for A_0 Mode)

Intact	
feature I	feature II
0.1535	1.1392e-004
0.1594	1.1369e-004
0.2143	1.1272e-004
0.1982	1.1303e-004
0.1815	1.139e-004
0.1955	1.1361e-004
0.2284	1.1288e-004
0.1407	1.1377e-004
0.1591	1.1311e-004
0.1173	1.1379e-004

Damage 1	
feature I	feature II
0.2294	1.1126e-004
0.2458	1.1223e-004
0.2499	1.1176e-004
0.1991	1.1181e-004
0.1755	1.1152e-004
0.2136	1.1216e-004
0.2383	1.1164e-004
0.1829	1.1189e-004
0.2446	1.1137e-004
0.2574	1.1144e-004

Damage 2	
feature I	feature II
0.6819	1.1129e-004
0.6915	1.1161e-004
0.8356	1.1089e-004
0.7208	1.1201e-004
0.5663	1.1173e-004
0.8865	1.1104e-004
0.8255	1.1178e-004
0.5979	1.1122e-004
0.6999	1.1095e-004
0.7912	1.1117e-004

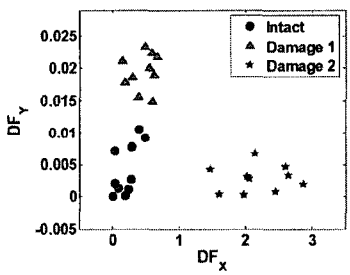

2-D Damage Feature Space

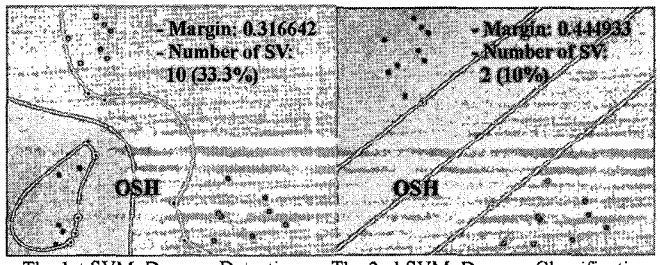

The 1st SVM: Damage Detection The 2nd SVM: Damage Classification

Figure 10. Establishment of Optimal Separable Hyper-planes by Two-Step SVM Classifier

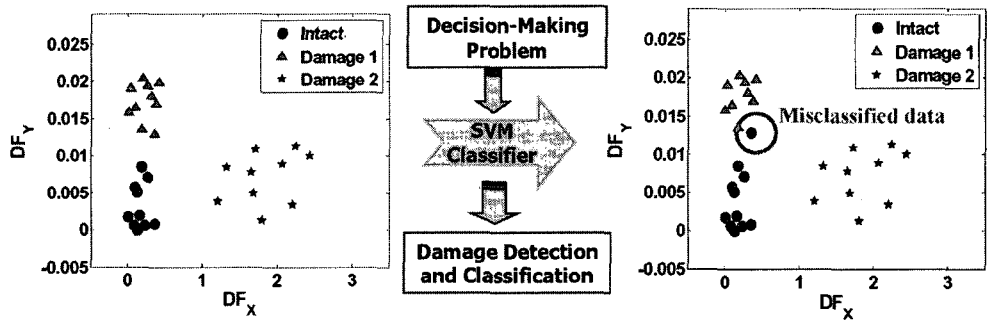

(Original Target Values) (SVM-based Estimation Values)

Figure 11. Damage Identification on Two-Dimensional Damage Feature Space
(Damage Estimation Rate of 96.67%)